



Theoretical study of Ce^{2+} cubic centres in alkaline earth fluoride crystals



N. Popov ^{a, b, *}, A. Mysovsky ^{a, b}, R. Shendrik ^b, E. Radzhabov ^b

^a Irkutsk National Research Technical University, 83 Lermontov Street, Irkutsk, Russia

^b A.P. Vinogradov Institute of Geochemistry SB RAS, 1a Favorsky St., Irkutsk, Russia

HIGHLIGHTS

- Ab initio study of Ce^{2+} impurity centres in alkaline earth fluoride crystals.
- Calculated Ce^{2+} ground state in CaF_2 and SrF_2 is predominantly $4f^15d^1$ singlet.
- Calculated absorption spectra are in good agreement with experimental data.

ARTICLE INFO

Article history:

Received 28 October 2015

Received in revised form

14 December 2015

Accepted 8 January 2016

Available online 12 January 2016

Keywords:

Rare earth

Cerium

Divalent

Spinorbit

QMMM

Quantum chemistry

ABSTRACT

In this paper we present theoretical study of Ce^{2+} impurity centres in alkaline earth fluoride crystals (CaF_2 , SrF_2). Only cubic configurations of centres were considered. Electronic levels and related properties were studied using CASSCF/CASPT2 approach within embedded-cluster formalism including scalar relativistic corrections and spin-orbital interaction. Calculated absorption spectra for Ce^{2+} in CaF_2 and SrF_2 are in good agreement with experimental data. For both crystals the ground state of Ce^{2+} ion has predominantly $4f^15d^1$ singlet character.

© 2016 Elsevier Ltd. All rights reserved.

1. Introduction

Alkaline earth fluorides (CaF_2 , SrF_2 , BaF_2) activated with trivalent rare earth ions are widely used as the material of scintillators. However, the same impurities can appear in alkaline earth fluoride crystals in divalent form upon additive colouration or irradiation and participate in energy transfer processes (Shendrik et al., 2016; McClure and Kiss, 1963; Merz and Pershan, 1967). The presence of divalent rare-earth ions might lead to the delay of scintillation process and decrease of the crystal light output.

It is well established that the divalent cerium free-ion ground state has 3H_4 $4f^2$ configuration and the lowest $4f^15d^1$ levels lie between 3277 and 18,444 cm^{-1} (Sugar, 1965). However, in the

crystal the interaction between crystal-field and many-electron wave-function can lower the energy of $4f^15d^1$ states compared to that of $4f^2$ states. Several authors have previously deduced that the ground state of cubic Ce^{2+} centres in CaF_2 is $4f^15d^1$ using ab initio methods (Visser et al., 1993) and crystal field theory calculation compared with experimental data (Alig et al., 1969). At the moment, theoretical works about electronic and geometrical structure as well as $4f^15d^1 \rightarrow 4f^2$ transitions of Ce^{2+} centres in SrF_2 crystals are not available. Experimental absorption spectrum of Ce^{2+} in SrF_2 has been obtained recently by our colleagues. Detailed information of this experimental can be founded in Ref. (Shendrik et al., 2016).

In order to achieve better understanding of the energy transfer process in alkaline earth fluorides further investigation of such centres is necessary. The purpose of this work is to investigate the structure, electronic configuration and electronic transitions for Ce^{2+} in CaF_2 and provide new theoretical results for Ce^{2+} in SrF_2 .

* Corresponding author. Irkutsk National Research Technical University, 83 Lermontov Street, Irkutsk, Russia.

E-mail address: brodiaga38@gmail.com (N. Popov).

2. Calculation details

Electronic structure calculations of cubic Ce^{2+} centres in CaF_2 and SrF_2 were performed with Molcas quantum chemistry package (Aquilante et al., 2010). Combined quantum mechanics/molecular mechanics (QMMM) embedded cluster approach which we used in this work allows us to divide the crystal with the defect into several regions described at different levels of theory:

1. Quantum-mechanical (QM) cluster which is calculated ab initio
2. Classical region where the interaction between ions is described with pair potentials
3. Region of fixed point charges reproducing proper crystalline field inside 1 + 2 region.

Using geometry optimization procedure we can obtain lattice polarization under defect presence. Lattice relaxation in this scheme is allowed for both classical and QM regions. Classic molecular mechanics interaction were described by Buckingham pair potentials. Parameters for Buckingham potential were obtained from Stoneham and Taylor (1981) and optimized for our model systems. This scheme has already shown good results in the works of various authors (Myasnikova et al., 2010; Mysovsky et al., 2011, 2004; Sushko et al., 2005).

Electronic structure calculations were performed at the state – average completed active space level of theory (SA-CASSCF).

ANO-RCC all electron basis sets were used for Ce (Roos et al., 2008), Ca (Roos et al., 2004) and Sr (Roos et al., 2004) ions. Ab initio model potentials (AIMPs) were placed on Ca, F (Pascual and Seijo, 1995) and Sr (Pascual et al., 2007) ions in the classical region in order to avoid possible distortion of QM cluster electronic density caused by the presence of bare Coulomb potentials created by point charges. Correlation of rare earth electronic states was taken into account using complete active space second order perturbation theory (CASPT2) (Andersson et al., 1990).

We decided to use such combination of electronic structure calculation methods because heavy elements (rare earth) exhibit strong static and dynamic correlation effects as a consequence of having a number of near degenerate electronic configurations. This combination shows good results in calculation of rare earth electronic structure (Ning et al., 2012).

SA-CASSCF spin-free calculations with 12 active orbitals (4f, 5d) and 2 active electrons performed with equal weight for all states provided the following state list (the absence of spin values in the term means this term appears for both singlet and triplet states):

- 1) $4f^15d^1$ with 5d electron belonging to E_g irreducible representation: $T_{1u} + T_{2u}, T_{1u} + T_{2u}, E_u$
- 2) $4f^15d^1$ with 5d electron belonging to T_{2g} irreducible representation: $T_{2u}, A_{2u} + E_u + T_{1u} + T_{2u}, A_{1u} + E_u + T_{1u} + T_{2u}$
- 3) $4f^2$ electrons in the same irreducible representation: ${}^3T_{1u} + {}^3T_{2u} + {}^3T_{3u}, 2 \times {}^1T_{1u} + 2 \times {}^1T_{2u} + {}^1A_{1u}$.
- 4) $4f^2$ electrons in the different irreducible representation: $A_{2g} + E_g + T_{1g} + T_{2g}, T_{1g}, T_{2g}$
- 5) $5d^2$ electrons in the same irreducible representation: ${}^3T_{2g}, {}^3E_g, 2 \times {}^1T_{2g}, 2 \times {}^1E_g$
- 6) $5d^2$ electrons in different irreducible representation: $T_{1g} + T_{2g}$

Absorption spectrum was obtained for a set of correlated states including spin–orbit interaction with the restrictive active space state interaction method (RASSI). In our model system spin–orbit coupling does not affect structural parameters of the defect and is ignored during structure relaxation process.

We have studied cubic configuration of the Ce^{2+} centres in CaF_2 and SrF_2 represented by the smallest possible $(\text{CeF}_8)^{5-}$ quantum

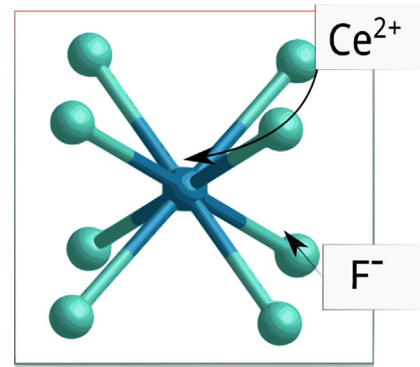


Fig. 1. $(\text{CeF}_8)^{5-}$ quantum cluster, Ce^{2+} at the centre and nearest neighbour F^- .

cluster (see Fig. 1). Geometry optimization was performed in O_h symmetry.

We have already used the same QMMM/CASPT2/RASSI combination of electronic structure methods in our previous work for Ce^{3+} O_h and C_{4v} centre in CaF_2 and obtained a good agreement with experimental data (Popov et al., 2015).

3. Result and discussion

3.1. Electronic and geometric properties

The distance between impurity Ce^{2+} ion and its nearest neighbours slightly increased during the geometry optimization of the defect ground state (See Table 1). As it was mentioned earlier the interaction of 5d E_g electron and the crystal field can lead to difference between free-ion and ion-in-the-crystal ground state electronic configuration. We obtained that the ground state of Ce^{2+} in both crystal is predominantly singlet $4f^15d^1$. Spin–orbit interaction leads to the ground state with the larger amount of singlet (80%) and small admixture of triplets states (20%). It is consistent with previous results for Ce^{2+} in CaF_2 where the ground state is mixture of ${}^1G_4 + {}^3F_3 + {}^3H_4$.

The lowest 14 spin-free states are $4f5d$ for both spin multiplicities. The character of lowest $4f^15d^1$ spin–orbit states in CaF_2 agree qualitatively with the results of crystal field calculation (Alig et al., 1969). Energies of these levels are shown in the first column of Table 2. The same energies with systematic error subtracted (around 600 cm^{-1}) are shown in column 4 as “Corrected”.

It should be noted that absorption spectrum can be obtained only if all considered states are included in the same state-averaged CASSCF calculation. The specifics of state-averaged CASSCF method is, simply speaking, that the more states are included in the calculation the worse is the accuracy of each particular state. The reason of energies overestimation in all-state averaging calculation is the intruder state inclusion, i.e. small admixture of some higher energy state.

This is why the energies obtained in such calculation turned out to be overestimated with respect to experiment by approximately 600 cm^{-1} for $4f^15d^1$ and by 4000 cm^{-1} for $4f^2$. In order to explain the nature of this systematic error we applied different state averaging schemes. Column 2 of Table 2 shows the energies of

Table 1
Nearest neighbour $\text{Ce}^{2+} - \text{F}^-$ distance before and after geometry optimization.

System	Before, Å	After, Å
Ce^{2+} in CaF_2	2.60	2.69
Ce^{2+} in SrF_2	2.77	2.81

Table 2
Energy levels (in cm^{-1}) of Ce^{2+} in CaF_2 , Δ SEC-systematic error correction.

State averaging		Δ SEC	Corrected	Expt. (Alig et al., 1969)	
All	Separate				
$4f^{15}d^1$:					
0(T_2)	0(T_2)	600	0(T_2)	0(T_2)	
850(E)	140(E)		250(E)	192(E)	
980(T_2)	340(T_2)		380(T_2)	427(T_2)	
1610(A_2)	984(A_2)		1010(A_2)	1074(A_2)	
1720(T_1)	1232(T_1)		1120(T_1)	1089(T_1)	
2250(E)	1730(E)		1650(E)	1488(E)	
2283(T_1)	1756(T_1)		1683(T_1)	1686(T_1)	
2700(A_2)	2214(A_2)		2100(A_2)	1831(A_2)	
$4f^2$:					
11,000(T_2)	7086(T_2)		4000	7000(T_2)	7011(T_2)
11,400(E)	7560(E)	7400(E)		7479(E)	
11,450(T_1)	7633(T_1)	7450(T_1)		7520(T_1)	
11,715(A_1)	7802(A_1)	7715(A_1)			
12,825(T_1)	8756(T_1)	8825(T_1)		8818(T_1)	
12,950(T)	8822(T_1)	8950(T_1)		8954(T_1)	
13,130(E)	9104(E)	9130(E)		9174(E)	
13,410(T_1)	9222(T_1)	9410(T_1)		9320(T_1)	

$4f^{15}d^1$ states with state averaging only over those states, as well as the energies of $4f^2$ states with averaging again only over this group of states. All these energies demonstrate excellent agreement with the experiment.

It can be observed from comparison of column 1 (all-state averaging) and column 2 (separate averaging over $4f^{15}d^1$ and $4f^2$ groups of states) that the order of states and their relative positions are the same. The energies obtained with all-state averaging can be corrected by subtraction of Δ SEC (systematic error correction) which is also shown in Table 2.

Concerning $4f^2$ one can see that lowest levels are described as 3H_4 with $T_2 + E + T_2 + A_1$ and 3H_5 with $T_1 + E + T_2 + T_1$. Splitting between these terms is around 2000 cm^{-1} . Next set of calculated levels (3H_6) appear before $10,000 \text{ cm}^{-1}$. Energy of such lowest levels were introduced in Table 2 for CaF_2 including systematic error subtraction (around 4000 cm^{-1}). Characteristic splitting of $4f^{15}d^1$ $E_g - T_{2g}$ is around $11,000 \text{ cm}^{-1}$. It was observed that lowest $5d^2$ state appears above $35,000 \text{ cm}^{-1}$ for Ce^{2+} in CaF_2 .

Similar calculations were performed for Ce^{2+} in SrF_2 . The resulting structure of energy levels is the same as in the case of CaF_2 . Calculated energy levels are presented in Table 3 for $4f^{15}d^1$ and $4f^2$. The only difference is that for SrF_2 the obtained energies are lower than for CaF_2 due to larger nearest neighbour distance. The $4f^2$ states in SrF_2 lie by 1000 cm^{-1} lower than in CaF_2 . Characteristic splitting of $4f^{15}d^1$ $E_g - T_{2g}$ is around $10,000 \text{ cm}^{-1}$. The lowest $5d^2$ state for Ce^{2+} in SrF_2 appears above $32,000 \text{ cm}^{-1}$.

3.2. Absorption spectrum

Calculated absorption and experimental data from Shendrik

Table 3
 $4f^{15}d^1$ and $4f^2$ energy levels (in cm^{-1}) of Ce^{2+} in SrF_2 .

$4f^{15}d^1$ calc.	$4f^2$ calc.
0(T_2)	6070(T_2)
300(E)	6150(E)
420(T_2)	6600(T_1)
1060(A_2)	6940(A_2)
1150(T_1)	8100(T_1)
1650(E_2)	8200(E)
1735(T_1)	8540(T_2)
1800(A_2)	8640(T_1)

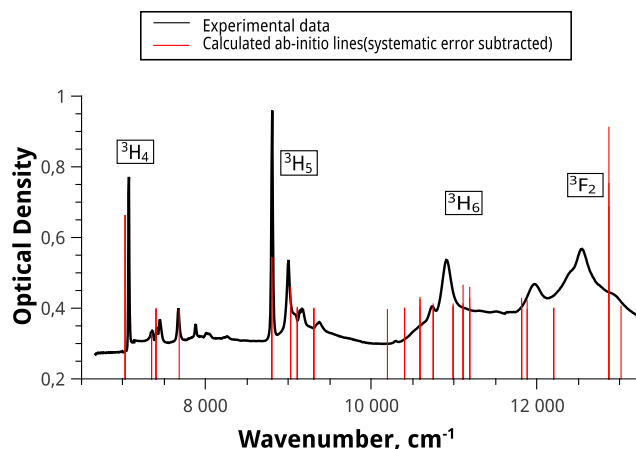


Fig. 2. Ce^{2+} cubic centre in CaF_2 optical absorption spectrum ($4f^{15}d^1 \rightarrow 4f^2$).

et al. (2016) spectra are shown in Fig. 2 for Ce^{2+} in CaF_2 and in Fig. 3 for SrF_2 . Calculated oscillator strengths have been renormalized to compare better with experimental data. Highest calculated oscillator strength for CaF_2 is 10^{-3} and SrF_2 is 5×10^{-4} .

As it was introduced in Refs. (Shendrik et al., 2016) and (Sizova and Radzhabov, 2012) for divalent cerium in CaF_2 one can observe two sets of absorption lines after x-ray irradiation in region of interest. There are: $6452, 9679, 10,490 \text{ cm}^{-1}$ narrow bands and $16,940, 22,580 \text{ cm}^{-1}$ wide bands. Narrow bands correspond $4f^{15}d^1 \rightarrow 4f^2$ transitions and the wide band is associated with photochromic PC^+ – centre (Sizova and Radzhabov, 2012). For Ce^{2+} in SrF_2 at 80 K we have a few sharp lines around 8100 cm^{-1} and wide bands at $11,290$ and $18,550 \text{ cm}^{-1}$.

Comparing theoretically calculated and experimental spectra it can be concluded that narrow bands in both crystals are due to $4f^{15}d^1 \rightarrow 4f^2$ transitions.

4. Conclusion

In this paper we had shown that divalent cerium centres can appear in CaF_2 and SrF_2 after additive colouration or x-ray irradiation. Using quantum chemistry calculation within embedded cluster formalism we have established that the ground state of cubic rare-earth defect is $4f^{15}d^1$ and has predominantly singlet character in with some triplet admixture.

The correct quantum-chemical description of these defects

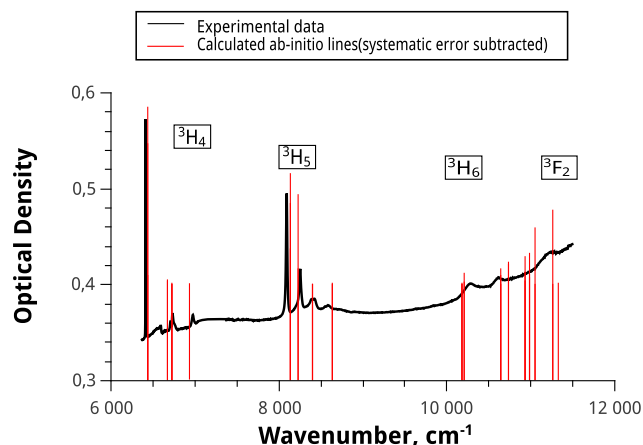


Fig. 3. Ce^{2+} cubic centre in SrF_2 optical absorption spectrum ($4f^{15}d^1 \rightarrow 4f^2$).

requires accounting for the dynamic correlation, scalar relativistic, spin-orbital and lattice polarization effects. Using this treatment we confirmed previous results of crystal-field and ab initio calculations (Visser et al., 1993) of cubic $Ce^{2+} O_h$ centre in CaF_2 and obtained new results for $Ce^{2+} O_h$ in SrF_2 . Experimentally obtained narrow absorption lines for cubic Ce^{2+} in CaF_2 and SrF_2 are in good agreement with calculated $4f^1 5d^1 \rightarrow 4f^2$ transition spectrum.

Acknowledgement

The reported study was funded by RFBR according to the research project No.15-02-06666_a.

All calculations were performed on a Fock supercomputer at Irkutsk National Research Technical University.

References

- Alig, R.C., Kiss, Z.J., Brown, J.P., McClure, D.S., 1969. Energy levels of Ce^{2+} in CaF_2 . *Phys. Rev.* 186, 276–284. <http://dx.doi.org/10.1103/PhysRev.186.276>. <http://link.aps.org/doi/10.1103/PhysRev.186.276>.
- Andersson, K., Malmqvist, P.A., Roos, B.O., Sadlej, A.J., Wolinski, K., 1990. Second-order perturbation theory with a CASSCF reference function. *J. Phys. Chem.* 94 (14), 5483–5488.
- Aquilante, F., De Vico, L., Ferré, N., Ghigo, G., Malmqvist, P.-å., Neogrády, P., Pedersen, T.B., Pitoňák, M., Reiher, M., Roos, B.O., et al., 2010. Molcas 7: the next generation. *J. Comput. Chem.* 31 (1), 224–247.
- McClure, D.S., Kiss, Z., 1963. Survey of the spectra of the divalent rare earth ions in cubic crystals. *J. Chem. Phys.* 39 (12), 3251–3257. <http://dx.doi.org/10.1063/1.1734186>. <http://scitation.aip.org/content/aip/journal/jcp/39/12/10.1063/1.1734186>.
- Merz, J.L., Pershan, P., 1967. Charge conversion of irradiated rare-earth ions in calcium fluoride. I. *Phys. Rev.* 162 (2), 217.
- Myasnikova, A., Radzhabov, E., Mysovsky, A., 2010. Ab initio calculation of charge-transfer absorption in CaF_2 and SrF_2 crystals with Eu^{3+} and Yb^{3+} impurities. *Nucl. Sci. IEEE Trans.* 57 (3), 1193–1195. <http://dx.doi.org/10.1109/TNS.2009.2035698>.
- Mysovsky, A.S., Sushko, P.V., Mukhopadhyay, S., Edwards, A.H., Shluger, A.L., 2004. Calibration of embedded-cluster method for defect studies in amorphous silica. *Phys. Rev. B* 69 (8), 085202.
- Mysovsky, A.S., Sushko, P.V., Radzhabov, E.A., Reichling, M., Shluger, A.L., 2011. Structure and properties of oxygen centers in CaF_2 crystals from ab initio embedded cluster calculations. *Phys. Rev. B* 84 (6), 064133.
- Ning, L., Wu, C., Li, L., Lin, L., Duan, C., Zhang, Y., Seijo, L., 2012. First-principles study on structural properties and 4f 5d transitions of locally charge-compensated Ce^{3+} in CaF_2 . *J. Phys. Chem. C* 116 (34), 18419–18426. <http://dx.doi.org/10.1021/jp305593h>. <http://dx.doi.org/10.1021/jp305593h>. <http://dx.doi.org/10.1021/jp305593h>.
- Pascual, J.L., Seijo, L., 1995. Ab initio model potential embedded cluster calculations including lattice relaxation and polarization: local distortions on Mn^{2+} -doped CaF_2 . *J. Chem. Phys.* 102 (13), 5368–5376.
- Pascual, J.L., Barandiarán, Z., Seijo, L., 2007. Relation between high-pressure spectroscopy and $f^{n-1}d^1$ excited-state geometry: a comparison between theoretical and experimental results in $SrF_2: Sm^{2+}$. *Phys. Rev. B* 76 (10), 104109.
- Popov, N.V., Radzhabov, E.A., Mysovsky, A.S., 2015. First-principles study of electronic structure of Ce^{3+} centres in alkaline-earth fluorides including spin-orbit and scalar relativistic effects. *IOP Conf. Ser. Mater. Sci. Eng.* 80 (1), 012025. <http://stacks.iop.org/1757-899X/80/i=1/a=012025>.
- Roos, B.O., Veryazov, V., Widmark, P.-O., 2004. Relativistic atomic natural orbital type basis sets for the alkaline and alkaline-earth atoms applied to the ground-state potentials for the corresponding dimers. *Theor. Chem. Acc.* 111 (2–6), 345–351. <http://dx.doi.org/10.1007/s00214-003-0537-0>. <http://dx.doi.org/10.1007/s00214-003-0537-0>.
- Roos, B.O., Lindh, R., Malmqvist, P.-Å., Veryazov, V., Widmark, P.-O., Borin, A.C., 2008. New relativistic atomic natural orbital basis sets for lanthanide atoms with applications to the Ce diatom and LuF_3 . *J. Phys. Chem. A* 112 (45), 11431–11435.
- Shendrik, R., Myasnikova, A., Radzhabov, E., Nepomnyashchikh, A., 2016. Spectroscopy of divalent rare earth ions in fluoride crystals. *J. Lumin.* <http://dx.doi.org/10.1016/j.jlumin.2015.06.055>. <http://www.sciencedirect.com/science/article/pii/S0022231315003890>.
- Sizova, T., Radzhabov, E., 2012. Photochromism in calcium and strontium fluoride crystals doped with rare-earths ions. *Nucl. Sci. IEEE Trans.* 59 (5), 2098–2101.
- Stoneham, A.M., Taylor, R., 1981. Handbook of Interatomic Potentials. Tech. rep. UKAEA Atomic Energy Research Establishment, Harwell. Theoretical Physics Div.
- Sugar, J., 1965. Description and analysis of the third spectrum of cerium (Ce III). *JOSA* 55 (1), 33–36.
- Sushko, P.V., Mukhopadhyay, S., Mysovsky, A.S., Sulimov, V.B., Taga, A., Shluger, A.L., 2005. Structure and properties of defects in amorphous silica: new insights from embedded cluster calculations. *J. Phys. Condens. Matter* 17 (21), S2115.
- Visser, R., Andriessen, J., Dorenbos, P., Van Eijk, C., 1993. Ce^{II} energy levels in alkaline-earth fluorides and cerium-electron, cerium-hole interactions. *J. Phys. Condens. Matter* 5 (32), 5887.